

POSITRON SPECTRUM OF Eu^{152} AND Eu^{152m}

S. F. ANTONOVA, S. S. VASILENKO, M. G. KAGANSKIĬ, and D. L. KAMINSKIĬ

Submitted to JETP editor April 18, 1959

J. Exptl. Theoret. Phys. (U.S.S.R.) **37**, 667-671 (September, 1959)

A low background β spectrometer was employed to study the spectrum of positrons produced in the decay of Eu^{152} and Eu^{152m} . It was found that β^+ decay of Eu^{152} takes place to the first (2^+) and second (4^+) excited states of Sm^{152} . The end-point energies of the partial spectra are 713 keV and 470 keV and their intensities are respectively 1.4×10^{-4} and 5×10^{-5} β^+ per decay. Formation of Sm^{152} in the ground and first excited states occurs in the positron decay of the Eu^{152m} isomer. The endpoint energies of the partial spectra are 890 keV and ~ 770 keV and the intensities are respectively 6×10^{-5} and 2×10^{-5} β^+ per decay. The excitation energy of the Eu^{152} isomer is deduced from the difference of the endpoint energies of the β^+ spectra and is found to be (55 ± 6) keV. Pair conversion coefficients and the multiplicities of a number of γ transitions are derived from the positron internal pair conversion spectra.

1. INTRODUCTION

It is known that a change in the number of neutrons in a nucleus from $N = 88$ to $N = 90$ also involves an abrupt change in the form of the nucleus. Therefore it is of considerable interest to study radioactive Eu^{152} and its isomer Eu^{152m} , which decay to ${}_{62}\text{Sm}_{90}^{152}$ and ${}_{64}\text{Gd}_{88}^{152}$. Electron capture, β^- decay, and γ radiation have been comparatively well investigated for these nuclei. Less has been done to study the positron decay of Eu^{152} and Eu^{152m} . Grodzins and Kendall¹ detected β^+ decay of the isomer Eu^{152m} . Earlier Kaminskiĭ and Kaganskiĭ² showed the existence of β^+ decay of Eu^{152} . A more detailed study of the positron decay of Eu^{152} and Eu^{152m} shows that the data of references 1 and 2 must be substantially supplemented. When the present experiment was almost completed we became aware of some of the results of the work of Alburger, Ofer, and Goldhaber,³ which had not yet been published. In general, their results agree with ours.

2. EXPERIMENTAL METHOD

A magnetic spectrometer of the sector type with double focusing as shown schematically in Fig. 1 was used to study the positron spectrum. The spectrometer used in our experiment is different from the detector described in reference 2. As can be seen in Fig. 1 the detector consists of two Geiger counters situated one meter from each other and connected to a coincidence circuit. The first counter was placed at the focus of the spectrometer.

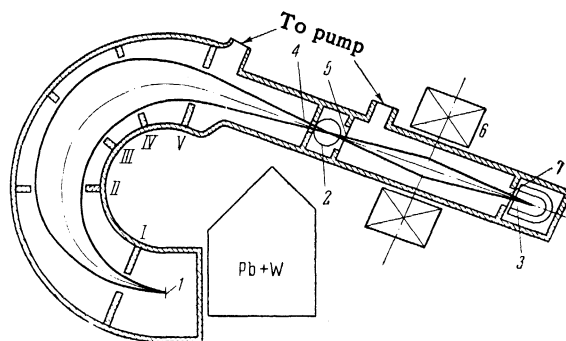


FIG. 1. Design of the β spectrometer. 1 – source; 2 and 3 – Geiger counters; 4, 5 and 7 – collodion films 0.2 mg/cm^2 ; 6 – magnetic lens; I to V – baffles.

β particles passing through the first counter were then focused with a magnetic lens on the second counter. The real advantage of such a counting system is the combination of a very small background and efficient detection of charged particles. The dependence of the detector efficiency on the energy of the particles is shown in Fig. 2 (by efficiency we mean the ratio of the number of coinci-

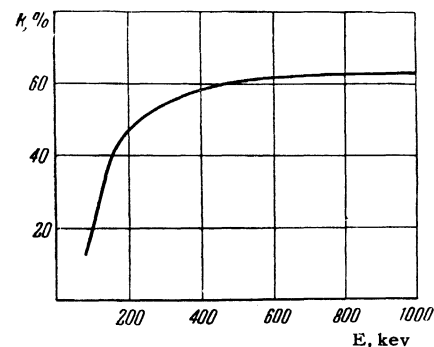


FIG. 2. Dependence of efficiency on β -particle energy.

dences to the number of pulses registered by the first counter). This dependence on energy resulted from the scattering of β particles in the first counter and in the films that separate the Geiger counters from the vacuum chamber.

In measuring the positron spectrum of Eu^{152} and $\text{Eu}^{152\text{m}}$ the spectrometer background was 2 to 3 orders lower than the intensity of the spectra being studied. The solid angle of the spectrometer was 0.5% of 4π and the resolution was 1%.

The sources used were obtained from europium oxide of a natural isotope compound irradiated by slow neutrons. The sources were prepared by precipitation from an emulsion and were 1 to 2 mg/cm^2 . In control experiments we used thinner sources, 0.2 mg/cm^2 which were prepared by electrolysis of europium chloride.⁴

3. RESULTS

Results of the measurements of the positron spectra of $\text{Eu}^{152,154}$ are shown in Fig. 3, which includes the correction for the dependence of the detector efficiency on positron energy. As can be seen from Fig. 3 the positron spectra are very complex. Sharp breaks in the spectrum at $H_\rho = 1920$ gauss cm and $H_\rho = 2460$ gauss cm are evidently caused by internal pair conversion of γ quanta with the energies $E_\gamma = 1280$ keV and $E_\gamma = 1409$ keV.

Insofar as the energy distribution of pair conversion positrons is known,* the corresponding spectra (a and b in Fig. 3) can be separated by the size of the break. After subtracting the pair conversion spectra the remaining spectrum was analyzed with a Fermi plot. Analysis shows that this spectrum consists of two β^+ -groups having the allowed shape with end-point energies of (713 ± 3) keV and (470 ± 10) keV. These partial β^+ spectra are shown in Fig. 3 (c and d).

Our measurements were taken several years after the irradiation of the sources. An attempt to evaluate the half-life of the positron spectrum gave the value ~ 10 years. In accordance with data in reference 2, this means that the positron spectrum shown in Fig. 3 is determined by the decay of the long-lived isotopes of Eu^{152} and Eu^{154} . In accordance with available data in reference 6, γ quanta with the energy $E_\gamma = 1280$ keV and consequently one of the pair conversion spectra arise from the decay of Eu^{154} . The other spectrum of pair conversion positrons is connected with the

*The pair conversion spectrum of positrons in our case, $Z = 62$ to 64, was assumed the same as for $Z = 84$ for which Jaeger and Hulme did the calculation.⁵

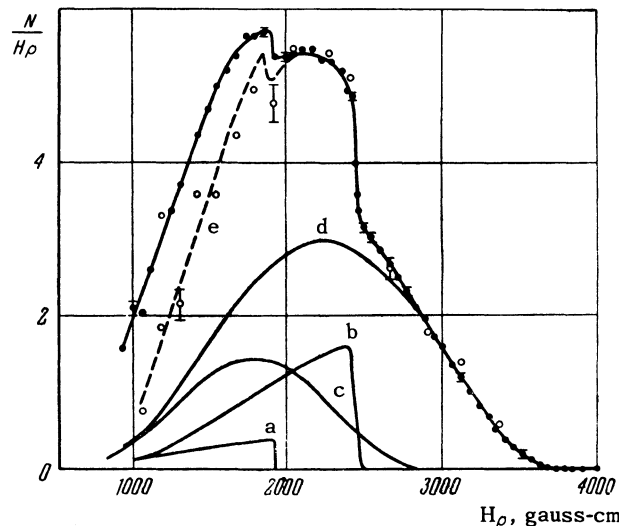


FIG. 3. Positron spectrum of $\text{Eu}^{152,154}$ measured with source thickness of 2 mg/cm^2 . Curve e is a sum spectrum of the four components. Points on curve e are the result of measurements with a source 0.2 mg/cm^2 thick.

1409-keV transition and results from the decay of Eu^{152} . Both β^+ spectra must be ascribed to the positron decay Eu^{152} to Sm^{152} since the difference between end point energies of these groups agrees perfectly with the energy separation between the first and second excited states of Sm^{152} .

Figure 4 shows the decay scheme of Eu^{152} which includes the data on positron decay obtained in our experiments. The intensities of partial β^+ groups were determined by comparing the corresponding spectra with the pair conversion spectrum associated with the 1409-keV transition. The probability of the 1409-keV transition in accordance with available data is taken equal to 25% (see Fig. 4), while the pair conversion coefficient was determined by the method described in reference 2, from the ratio of the areas of the spectra of K-electron conversion and positron pair conversion. The value of the pair conversion coefficient is Γ

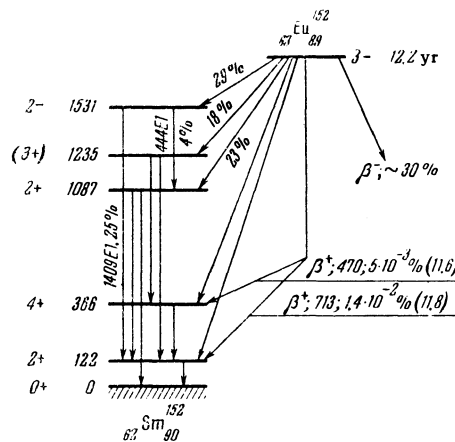


FIG. 4. Decay of Eu^{152} to Sm^{152} .

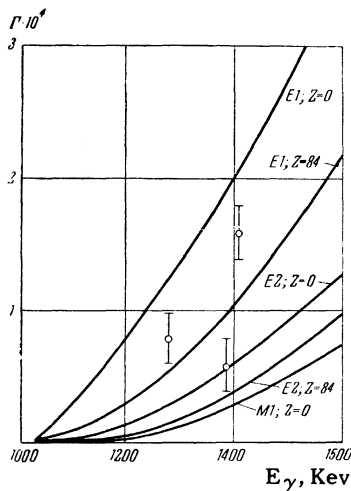


FIG. 5. Dependence of the pair-conversion coefficient on the energy and multipolarity of transition. Points are the result of our measurements.

$= (1.6 \pm 0.2) \times 10^{-4}$ as can be seen in Fig. 5, and agrees with the multipolarity E1 established for this transition by other methods. The pair conversion coefficient $\Gamma = (0.8 \pm 0.2) \times 10^{-4}$ for the 1280-keV transition also corresponds to a multipolarity E1. Thus for the calculation of Γ the relative intensity of this γ transition was taken equal to $I_{1280} = 0.35 I_{1409}$ in agreement with data given by Dzhelepov and others.⁷

After separating from the spectrum the four components shown in Fig. 3 there remains a surplus of positrons in the energy region below 250 keV. Control measurements carried out with a considerably thinner source (0.2 mg/cm^2) showed that this surplus was caused by scattering in the comparatively thick sources used in the basic measurements. Results of these measurements are shown in the same figure.

In our experiments the positron decay of Eu^{154} was not detected. However, on the basis of available data on the mass difference of Eu^{154} and Sm^{154} we can assume the presence of β^+ decay of Eu^{154} with an end-point energy of $\sim 1 \text{ MeV}$. According to our experiments the probability of such a decay is less than 10^{-6} positron per decay of $\text{Eu}^{152,154}$.

Figure 6 shows the results of measurements of the positron spectrum of the $\text{Eu}^{152\text{m}}$ isomer. Measurement of the half-life of this spectrum gave the value $T_{1/2} = 9.2$ hours. In contrast to the positron spectrum of Eu^{152} (in Fig. 3), there are few positrons here which result from pair conversion. The fact that in the decay of the 9.2-hour isomer, the γ transitions with an energy of more than 2 mc^2 are comparatively weak confirms this. We made a more detailed study of spectra in the 380-keV energy region. The measurements showed (see Fig. 6) the presence of a small break at 364 keV which corresponds to the γ -transition energy $E_\gamma = 1386 \text{ keV}$. Calculation

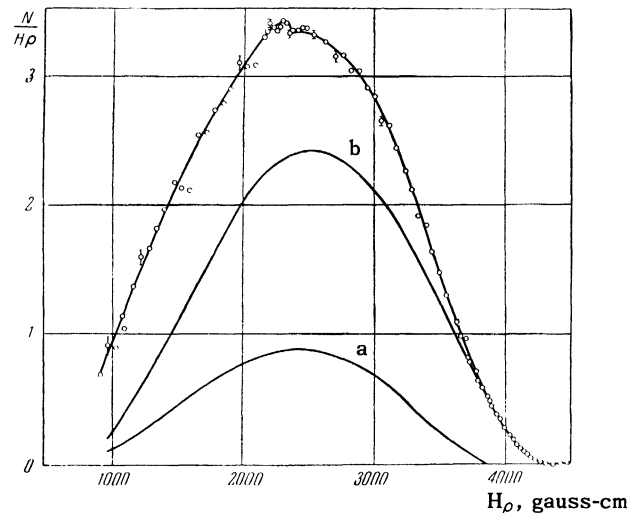


FIG. 6. Positron spectrum of $\text{Eu}^{152\text{m}}$. Source thickness 1.5 mg/cm^2 .

of the pair conversion coefficient for this transition gave the value $\Gamma = (0.6 \pm 0.3) \times 10^{-4}$, which gives a multipolarity E2 (see Fig. 5); for the calculation the intensity of the γ quanta was taken as equal to 0.7% to correspond with Marklund's data.⁸

An analysis of the β^+ -spectrum, using the Fermi plot method, showed the presence of two components of β^+ decay with the energies $(890 \pm 5) \text{ keV}$ and $\sim 770 \text{ keV}$. These components were identified as the positron decays of $\text{Eu}^{152\text{m}}$ to the ground and first excited states of Sm^{152} . Figure 7 shows the decay scheme of the 9.2-hour isomer (according to Marklund's data⁸) which includes the results obtained in our work. The intensity of the β^+ spectrum was determined from the ratio of the areas of the positron and electron spectra. Inasmuch as the value for the spin of the isomeric state still remained undetermined (0^- or 1^-) it was of considerable interest to determine the form

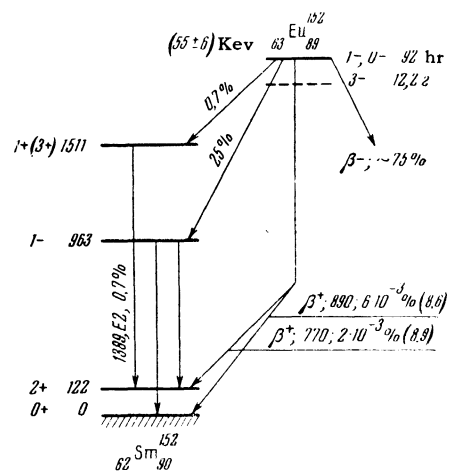


FIG. 7. Decay of $\text{Eu}^{152\text{m}}$ to Sm^{152} .

	Alburger et al. ³		Our data	
	End-point energy, kev	Intensity, β^+ per decay	End-point energy, kev	Intensity, β^+ per decay
Eu ¹⁵²	715±10 470±30	1.6·10 ⁻⁴ 0.8·10 ⁻⁴	713±3 470±10	(1.4±0.2)·10 ⁻⁴ (0.5±0.1)·10 ⁻⁴
Eu ^{152m}	895±5 ~770	7·10 ⁻⁵ 4·10 ⁻⁵	890±5 770±30	(6±1)·10 ⁻⁵ (2±0.5)·10 ⁻⁵

of the β^+ spectrum corresponding to the decay of Eu^{152m} to the first excited state of Sm¹⁵². The unique form for the spectrum would give for the spin of Eu^{152m} the value 0⁻. However, the attempt to establish the form of the spectrum in our work was unsuccessful because of the comparatively small difference between the end-point energies of the components (120 kev) and consequently a certain arbitrariness in separating them.

The table shows the data for positron decay of Eu¹⁵² and Eu^{152m} obtained by us and also by Alburger et al.³ As can be seen from the table, the results in reference 3 generally agree with our work. The only real difference is in the intensity of the low energy components. The reason for this is not yet clear since the experimental part of reference 3 has not yet been published. We determined the energy of the metastable state for the end point energies of β^+ decay of Eu¹⁵² and Eu^{152m}. Our data gives this energy as (55 ± 6) kev.

The authors wish to thank Professor L. A. Sliv for his constant attention and interest in our work.

¹H. Kendall and L. Grodzins, Bull. Am. Phys. Soc. Ser. II, **1**, 164 (1956).

²D. L. Kaminskiĭ and M. G. Kaganskiĭ, JETP **35**, 926 (1958), Soviet Phys. JETP **8**, 646 (1959).

³Alburger, Ofer, and Goldhaber, Phys. Rev. (in press); Phys. Rev. Lett. **1**, 479 (1958).

⁴B. V. Bobykin and K. M. Novik, Izv. Akad. Nauk SSSR, Ser. Fiz. **21**, 1556 (1957), Columbia Tech. Transl. p. 1546.

⁵J. C. Jaeger and H. R. Hulme, Proc. Roy. Soc. (London) **A148**, 703 (1935).

⁶B. S. Dzhelepov and L. K. Peker, Схемы распада (Decay Schemes), M. 1958.

⁷Dzhelepov, Zhukovskii, and Nedovesov, Izv. Akad. Nauk SSSR, Ser. Fiz. **19**, 296 (1955), Columbia Tech. Transl. p. 269.

⁸I. Marklund, Nucl. Phys. **9**, 83 (1958/1959).

Translated by Geneva Gerhart

131

Vacuum Tubes (see Methods and Instruments)

Viscosity (see Liquids)

Wave Mechanics (see Quantum Mechanics)

Work Function (see Electrical Properties)

X-rays

Anomalous Heat Capacity and Nuclear Resonance in Crystalline Hydrogen in Connection with New Data

on Its Structure. S. S. Dukhin — 1054L.

Diffraction of X-rays by Polycrystalline Samples of Hydrogen Isotopes. V. S. Kogan, B. G. Lazarev, and R. F. Bulatova — 485.

Investigation of X-ray Spectra of Superconducting CuS.

I. B. Borovskii and I. A. Ovsyannikova — 1033L.

Optical Anisotropy of Atomic Nuclei. A. M. Baldin — 142.

ERRATA TO VOLUME 9

On page 868, column 1, item (e) should read:

(e). Ferromagnetic weak solid solutions. By way of an example, we consider the system Fe-Me with A2 lattice, where Me = Ti, V, Cr, Mn, Co, and Ni. For these the variation of the moment m with concentration c is

$$dm/dc = (Nd)_{Me} \mp 0.642 \{ 8 (2.478 - R_{Me}) + 6 |2.861 - R_{Me}| \mp [8(2.478 - R_{Fe}) + 6(2.861 - R_{Fe})] \},$$

where the signs $-$ and $+$ pertain respectively to ferromagnetic and paramagnetic Me when in front of the curly brackets, and to metals of class 1 and 2 when in front of the square brackets. The first term and the square brackets are considered only for ferromagnetic Me. We then have $dm/dc = -3$ (-3.3) for Ti, -2.6 (-2.2) for V, -2.2 (-2.2) for Cr, -2 (-2) for Mn, 0.7 (0.6) for Ni, and 1.2 (1.2) for Co; the parentheses contain the experimental values.

ERRATA TO VOLUME 10

Page	Reads	Should Read
224, Ordinate of figure	10^{23}	10^{29}
228, Column 1, line 9 from top	3.6×10^{-2} mm/min	0.36 mm/min
228, Column 1, line 16 from top	0.5 mm/sec	0.05 mm/min
329, Third line of Eq. (23a)	$+ (1/4 \cosh r + \dots$	$+ 1/4 (\cosh r + \dots$
413, Table II, line 2 from bottom	$-0.0924 \pm$	$-1.0924 \pm$
413, Table II, line 3 from bottom	$+1.8730 \pm$	$+0.8370 \pm$
479, Fig. 7, right, 1st line	92 hr	9.2 hr
499, Second line of Eq. (1.8)	$+\tilde{k} \sin^2 \alpha / \omega_N^2 + \langle c^2 \tilde{k}^2 \dots$	$+\left(\tilde{k}/\omega_H\right)^2 \sin^2 \alpha \langle c^2 \tilde{k}^2 \dots$
648, Column 1, line 18 from top	18×80 mm	180×80 mm
804, First line of Eq. (17)	$-1/3 (\alpha_x^2 \alpha_y^2 + \dots$	$\dots - 3 (\alpha_x^2 \alpha_y^2 + \dots$
967, Column 1, line 11 from top	$\sigma(N', \pi) \approx 46(N', N')$	$\sigma(N', \pi) > \sigma(N', N')$
976, First line of Eq. (10)	$= \frac{e^2}{3r^2c^4}$	$= \frac{e^2}{3\hbar^2c^2}$
978, First line of Eq. (23)	$\left[\frac{(2\gamma^2 - 1)^2}{(\gamma^2 - 1) \sin^4(\theta/2)} \right]$	$\left[\frac{(2\gamma^2 - 1)^2}{(\gamma^2 - 1)^2 \sin^4(\theta/2)} \right]$